Hiaper HSRL performance report, 19-Sep-08

Table 1 compares the delievered specifications to those in our proposal. The delivered system closely matches the proposed system with only small differences. The delivered lidar is capable of transmitting an average power of approximately 1 W. However, for ground based operation, the power is limited to 500 mW in order to insure that the transmitted beam is safe for direct viewing. In downward looking airborne application the repetition rate can be increased to 6 kHz. This will decrease the energy in each laser pulse and make it possible to transmit slightly higher power and still be eyesafe. Higher repetition rates are not desirable in ground based and upward pointing operation because atmospheric scattering from the previous laser pulse at high altitudes contaminates the measurement of background light that is acquired just before the laser is fired. For the sake of system robustness and ease of alignment we selected fiber-coupled detectors; fiber losses slightly reduces the quantum efficiency of these detectors.

Table 1: Basic specifications:

	Proposed	Delivered	Notes
Average power	600 mW	>600 mW	Eyesafety limits ground-based output to 500 mW
Repetition rate	6 kHz	4 kHz	Can be increased to 6 kHz for airborne operation
Wavelength	532 nm	532 nm	
Solar noise bandwidth	6 GHz	6 GHz	Full-width half maximum bandwidth
Angular field-of-view	75 u-rad	63 u-rad	Installation of other field stops allow 45-85 u-rad
Telescope diameter	40 cm	40 cm	
Detectors	APD	APD	Perkin-Elmer SPCM-ARQ, Geiger-mode APDs
Quantum efficiency	>60%	50%	As supplied per Perkin-Elmer specifications
Data acquisition			Photon counting
Max range resolution	7.5 m	7.5 m	
Max time resolution	0.5 s	0.5 s	
Data export			Hard disk netcdf files and/or TCIP/IP export

The lidar has completed more than 3-months of nearly continuous operation in our roof-top laboratory. All data from this operation has been placed on a public web site (http://lidar.ssec.wisc.edu). Data is posted in real time as it is acquired. Quick look images and custom image generation software allows anyone to examine the data. Furthermore all of the data is available for download as netcdf files. These data files include both the raw data and the processed profiles of backscatter cross section, depolarization, and optical depth. All of the calibration data required for processing are also included. Extensive displays of system housekeeping data are provided so that the performance of subsystems can be studied in detail.

Figure 1 shows an example of the lidar data. This image shows the calibrated particulate backscatter cross section as a function of time and altitude measured on August 28, 2008. Molecular scattering has been removed from this data making very tenuous aerosol layers visible. Figure 2 shows the circular depolarization ratio observed at the same time. These images were selected because they show a range of atmospheric conditions and they demonstrate that the system is capable of the measurements described in our proposal. Features evident in the images include: 1) Before 7 UT stratospheric aerosol layers from the Kasatochi volcanic eruption in the Aleutian Islands are visible at altitudes between 17 and 19 km. The very low depolarization shown in figure 2 verifies that these layers are composed of spherical droplets. 2) A relatively dense layer of aerosols below 1 km marks the atmospheric boundary layer. The depolarization of this layer decreases with altitude due to the increased scattering from hygroscopic aerosols in the upper part of the boundary layer. These aerosols grow in size as the relative humidity increases and their scattering begins to dominate contributions from non-spherical aerosols. 3) An optically thin cirrus cloud between 10 and 13 km shows high depolarization (red areas in depolarization plot) characteristic of ice crystals. 4) A variety of tenuous aerosol layers with varying depolarizations are seen between 1 and 14 km before the dense clouds appear around 7 UT. 5) Beginning at 7 UT a base an optically dense ice cloud appears. Its base slowly descends from 12 to 6.5 km. 6) At 8:45 UT a water cloud showing the very low depolarizations characteristic of spherical particles appears at 3 km. 7) Rain showers are seen falling from the the 3 km cloud beginning at 9:20 and continuing to 11:30 UT. Aerodynamic drag distorts rain drops causing the depolarization of the rain to be larger than that of liquid cloud droplets.

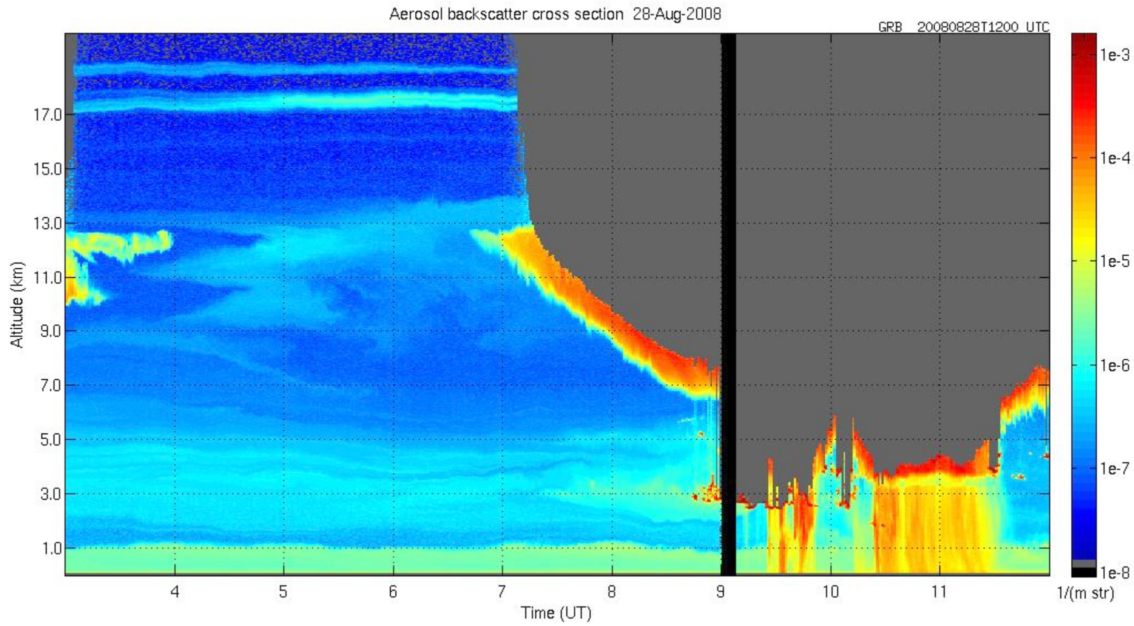

Figure 1: Backscatter cross section measured between 3 and 12 UT on August 28, 2008 showing a variety of atmospheric phenomena. A computer controlled system calibration is scheduled twice each day. It causes the dark vertical bar at 9 UT.

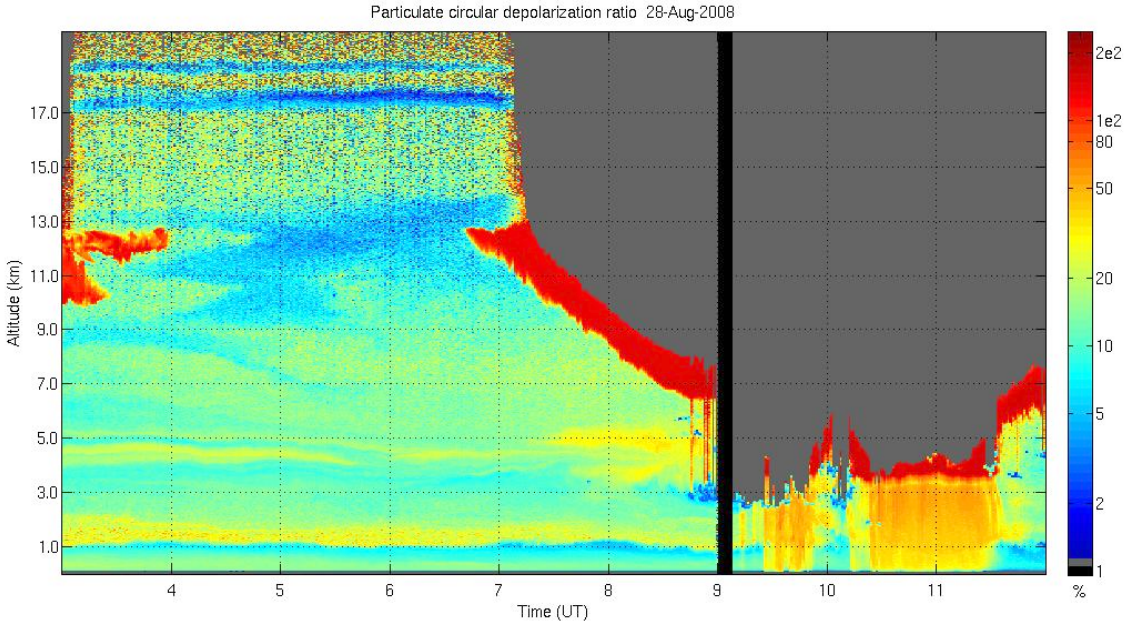

Figure 2: Circular depolarization measured between 3 and 12 UT on August 28, 2008.

Figure 3 shows a one-minute average optical depth measured on 14-Sept-2008. In this case, a water cloud below 400 m is shown to have an optical depth of 1.3 and dense ice cloud with a base at 3 km provides usable returns up to an altitude of 4.4 km before the lidar return is too weak to detect. At this point the optical depth is ~4 confirming the projected maximum penetrations projected in our proposal.